A three-dimensional boundary element model for the analysis of polycrystalline materials at the microscale

I. Benedetti[1,2,a], M.H. Aliabadi[1,b]

[1]Department of Aeronautics, Imperial College London, South Kensington Campus,SW7 2AZ, London, UK.

[2]Dipartimento di Ingegneria Civile, Ambientale, Aerospaziale e dei materiali, Università degli Studi di Palermo, Viale delle Scienze, Edificio 8, 90128, Palermo, Italy

[a]i.benedetti@imperial.ac.uk, [a]ivano.benedetti@unipa.it, [b]m.h.aliabadi@imperial.ac.uk

Keywords: Polycrystalline materials, Microstructure Modelling, Material Homogenization, Multi-region formulation, Anisotropic Boundary Element Method.

Abstract. A three-dimensional multi-domain anisotropic boundary element formulation is presented for the analysis of polycrystalline microstructures. The formulation is naturally expressed in terms of intergranular displacements and tractions that play an important role in polycrystalline micromechanics, micro-damage and micro-cracking. The artificial morphology is generated by Hardcore Voronoi tessellation, which embodies the main statistical features of polycrystalline microstructures. Each crystal is modeled as an anisotropic elastic region and the integrity of the aggregate is restored by enforcing interface continuity and equilibrium between contiguous grains. The developed technique has been applied to the numerical homogenization of SiC and the obtained results agree very well with available data.

Introduction

Macroscopic material properties depend on the material microstructure. Understanding the link between micro- and macro-properties is an important and technologically relevant task of modern Materials Science. The estimation of the effective material properties can be carried out at different levels [1]. A modern approach to material homogenization is the use of numerical models for the simulation of the material behavior at the microstructural scale [2].

Polycrystalline materials constitute an important class of heterogeneous materials [3]. Many engineering materials (metals, ceramics) present a polycrystalline microstructure. The internal structure of polycrystals is determined by the size and shape of the grains, by their crystallographic orientation and by different types of defects. A crucial role in the determination of the polycrystalline aggregate properties is played by the intergranular interfaces and their defects [4].

The polycrystalline microstructure can be investigated by using different experimental techniques [5,6]. These provide fundamental information but require sophisticated equipment, material manufacturing and preparation and complicated post-processing, resulting then generally expensive and time consuming. A viable alternative, or complement, to the experimental characterization is offered by Computational Micromechanics [2]. The dramatic increase in computational power and the formulation of reliable mathematical models allow to simulate the response of complex microstructures at little cost, thus complementing and accelerating the experimental campaigns when, for example, the design of a new material is pursued.

In the present study, a three-dimensional boundary integral formulation for the analysis of polycrystalline microstructures is presented. The technique is alternative to the more used FEM and its typical features are: a) the simplification in the artificial microstructure generation and modelling, especially in relation to the meshing of the artificial microstructure, since only the discretization of the grains surface is required; b) the microstructural problem is formulated

directly in terms of intergranular displacements and tractions, which play an important role in polycrystalline micromechanics, especially when damage and micro-cracking are involved [7].

Artificial microstructure

The artificial microstructure must retain the main topological, morphological and crystallographic features of the aggregate. For polycrystalline materials, Voronoi tesselations are widely used for the generation of the microstructural models [4,8,9]. The Voronoi cells are convex polyhedra bounded by flat polygonal convex faces. Voroni tessellations have the advantage of being analytically defined, relatively simple to generate and possess some features that make them suitable for numerical treatment, (straight edges and flat faces). Here the Hardcore Voronoi tessellation is adopted for generating the microstructure: the additional *hardcore* constraint produces more regular grains and tessellations.
The assignation of a specific orientation to each crystal of the aggregate completes the microstructure representation. In this work, each grain is assigned a random orientation from a uniform distribution in the group of rotations in the three-dimensional space.

Microstructure boundary element model

Material modelling. Each grain is modeled as a three-dimensional linear elastic orthotropic domain with arbitrary spatial orientation. This is not restrictive, as the majority of single metallic and ceramic crystals present general orthotropic behavior.
Grain boundary element formulation. Each crystal is modeled by using the Boundary Element Method (BEM) for 3D anisotropic elasticity [10]. The polycrystalline aggregate is seen as a multi-region problem, so that different elastic properties and spatial orientation can be assigned to each grain [11]. Given a volume bounded by an external surface and containing N_g grains, two kinds of grains can be distinguished: the *boundary grains*, intersecting the external boundary, and the *internal grains*, completely surrounded by other grains. Boundary conditions are prescribed on the surface of the boundary grains lying on the external boundary, while interface continuity and equilibrium conditions are forced on interfaces between adjacent grains, to restore the integrity of the aggregate. In general, the boundary integral equation for a generic grain $\mathcal{G}_k$ is written

$$c_{ij}^k(\boldsymbol{x})u_j^k(\boldsymbol{x}) + \int_{B_C \cup B_{NC}} T_{ij}^k(\boldsymbol{x},\boldsymbol{y})u_j^k(\boldsymbol{y})dB^k(\boldsymbol{y}) = \int_{B_C \cup B_{NC}} U_{ij}^k(\boldsymbol{x},\boldsymbol{y})t_j^k(\boldsymbol{y})dB^k(\boldsymbol{y}), \tag{1}$$

where u_i^k and t_i^k denote boundary displacements and tractions of the grain $\mathcal{G}_k$, and U_{ij}^k and T_{ij}^k represent the components of the 3D anisotropic displacement and traction fundamental solutions. The integrals appearing in Eq. 1 are extended over the entire surface of the grain, given by the union of *contact* surfaces B_C, in common with other grains, where interface conditions apply, and *non-contact* surfaces B_{NC}, where boundary conditions apply. Eq. 1 is complemented by the

$$\begin{cases} u_i^k = \overline{u}_i^k \\ t_i^k = \overline{t}_i^k \end{cases} \quad \textit{Boundary conditions} \qquad \begin{cases} \tilde{u}_i^k + \tilde{u}_i^j = \delta\tilde{u}_i^{kj} = 0 \\ \tilde{t}_i^k = \tilde{t}_i^j \end{cases} \quad \textit{Interface conditions}, \tag{2}$$

where the overbar denotes prescribed quantities, while the tilde represents quantities expressed in an interface local reference system, more suitable for the interface conditions. The interface conditions involve surface displacements and tractions from two different grains, $\mathcal{G}_k$ and $\mathcal{G}_j$.

After discretization and integration of Eq. 1 for each grain, the final system of equations for the aggregate can be written

$$\begin{bmatrix} \mathbf{A}_1 & \mathbf{0} & \mathbf{0} \\ \mathbf{0} & \ddots & \mathbf{0} \\ \mathbf{0} & \mathbf{0} & \mathbf{A}_{N_g} \\ & [\mathbf{I}] & \end{bmatrix} \begin{bmatrix} \boldsymbol{x}_1 \\ \vdots \\ \boldsymbol{x}_{N_g} \end{bmatrix} = \begin{bmatrix} \boldsymbol{y}_1 \\ \vdots \\ \boldsymbol{y}_{N_g} \\ \mathbf{0} \end{bmatrix}, \tag{3}$$

where the vectors $\boldsymbol{x}_k$ contain the unknown components of displacements and tractions, the matrix blocks $\mathbf{A}_k$ are the grain boundary element matrices, the matrix $\mathbf{I}$ contain the coefficients of the interface conditions and the terms $\boldsymbol{y}_k$ stem from the boundary conditions. System 3 is highly sparse and the use of specialized sparse solvers is then desirable to speed up the numerical solution.

Grain boundary element discretization. The presented formulation has the remarkable advantage that only meshing of the grains surfaces is required. The artificial microstructure is, in this context, a collection of flat convex polygonal faces. Plane triangular linear elements are used to discretize such faces. Constant or linear discontinuous triangular elements are implemented for representing the unknown boundary fields. The mesh generator Triangle (http://www.cs.cmu.edu/~quake/ triangle.html, [12]) is used for the creation of a two-dimensional high-quality mesh of each plane cell face. Since the Voronoi tessellations used for microstructure modelling have stochastic nature, care must be taken to ensure mesh consistency and homogeneity to the greatest extent. This is achieved by introducing a discretization parameter d_m governing the mesh density, so to create meshes as homogeneous as possible: d_m sets the number of segments in which the average length edge in the tessellation is subdivided into. Fig. 1 shows the mesh of a tessellation with 150 grains and the representative mesh of few single grains taken from the same tessellation.

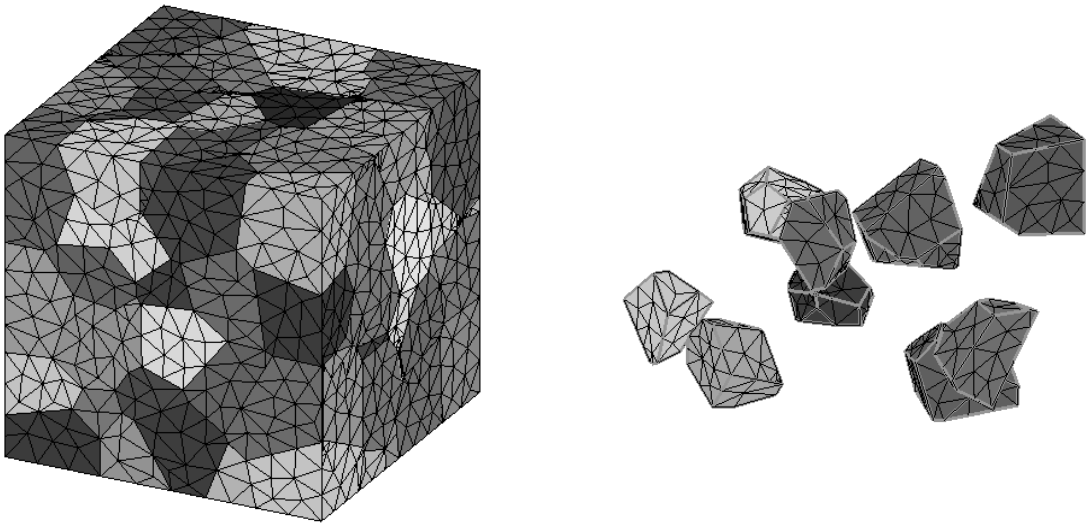

Figure 1: Mesh of a tessellation containing 150 grains and representative mesh of few grains.

Numerical estimation of elastic properties of SiC

Before proceeding with the determination of the effective properties of the considered polycrystals, the developed technique has been tuned in terms of mesh density and boundary element type. As already described, the mesh density is controlled by the parameter d_m. Moreover, in this work, two different types of elements have been implemented: *constant* elements and *discontinuous linear*

elements. To tune the method, a copper polycrystal with $N_g = 10$ grains is first analyzed. The material properties for the copper crystals are given in [8]. The aggregate is subjected to two different sets of linear displacement boundary conditions, the first enforcing a macro elongation Γ_{33} and the second enforcing a macro shear strain Γ_{13}. The convergence of the computed stress volume averages is checked, in order to set both mesh density d_m and element type for the subsequent set of computations. Enforcing Γ_{33} by means of linear boundary displacements allows to compute the third column of the apparent stiffness matrix $\hat{\mathbf{C}}$ for the aggregate, and in particular $\hat{C}_{13}$, $\hat{C}_{23}$ and $\hat{C}_{33}$. In the same way, by enforcing Γ_{13}, the fifth column of the apparent stiffness matrix can be evaluated, and in particular $\hat{C}_{55}$. The numerical convergence of such quantities is shown in Fig. 2. In the plot, the apparent quantities are normalized with respect to the homologous value obtained by using the most refined scheme, i.e. the finest mesh with linear discontinuous elements, so that the trend of the quantities $\hat{C}_{ij} / \hat{C}_{ij}^{ref}$ is shown. The linear scheme does not show a remarkable dependence on the mesh refinement for any considered apparent quantities, and the computed values can be considered converged even for the coarser mesh. The same behavior is noticed if constant traction boundary conditions are enforced and the components of the compliance matrix are evaluated, instead of the stiffness matrix. As a consequence, linear discontinuous elements with $d_m = 1$ will be used in the following computations.

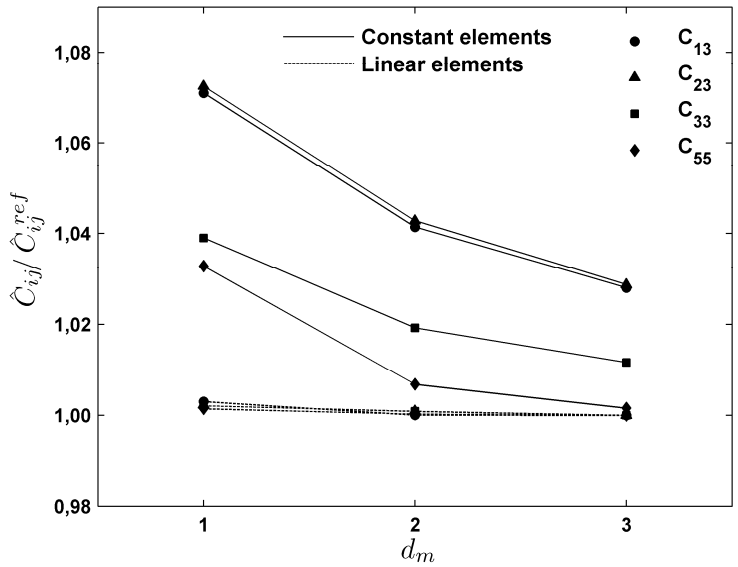

Figure 2: Convergence of apparent elastic properties with element type and mesh density.

After numerical tuning, the macroscopic effective properties of silicon carbide (SiC) are estimated. The performed analysis takes into account the stochastic nature of the microstructure, in terms of grain size, morphology and orientation. Aggregates with $N_g = 10$, 20, 50, 100 and 150 grains have been simulated and for each number of grains $N_R = 100$ realizations have been generated. Each realization differs from the others in terms of both geometry and crystallographic orientation. Given a polycrystalline realization, consisting of N_g grains and subjected to a given set of consistent boundary conditions, since the material is supposed to not develop microcracks, stress and strain volume averages can be used to extract the apparent elastic modula, see for example [1,2]. Kinematic uniform boundary conditions, i.e. linear displacement boundary conditions

corresponding to prescribed macro-strains, have been enforced on each simulated realization. Table 1 lists the elastic constants for hexagonal single crystal SiC, as measured by Arlt and Schodder [14]: these constants define the material of the single grains, which are then given a random orientation in the three-dimensional space. Fig. 3 shows the mean values and the scatter of the apparent Young's modulus and shear modulus over the considered number of realizations: since linear displacement BCs are applied, the apparent properties approach the effective ones from higher values; moreover, it is worth noting how the scatter decreases when an higher number of grains is considered. The values of the effective elastic modula *E* and *G* for polycrystalline SiC have been reported by various authors, see Lambrecht et al. [15] and references therein. In this study, the average values, calculated over $N_R = 100$ realizations of aggregates with $N_g = 150$ grains, are E=456 GPa and G=193 GPa, which are in very good agreement with the values E=448 GPa and G=192 GPa, reported by Carnahan [16], who used low porosity samples and extrapolated the values to zero porosity. The average computed value of the Poisson ratio was $\nu = 0.181$, close to the value $\nu = 0.168$ yielded by Carnahan estimations.

C_{11}	C_{12}	C_{13}	C_{33}	C_{44}	C_{66}
502	95	96	565	169	203.5

Table 1: Elastic constants for hexagonal single-crystal SiC [Gpa].

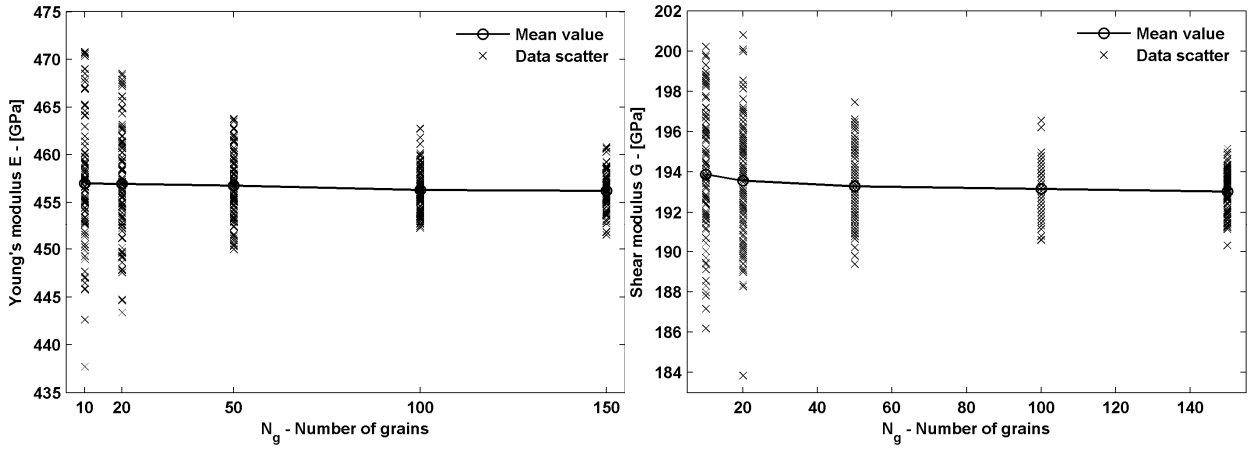

Figure 3: Apparent properties of SiC against number of grains in the simulated aggregate.

Summary

A three-dimensional boundary element formulation for the analysis of polycrystalline microstructures has been developed. The technique allows a remarkable simplification in the generation of the artificial microstructure model and it is directly formulated in terms of intergranular displacements and tractions, which play an important role in polycrystalline micromechanics. The developed method has been applied to the determination of the effective properties of silicon carbide and the results have shown remarkable agreement with literature data in the framework of numerical homogenization.

Acknowledgements

This research was supported by a Marie Curie Intra European Fellowship within the 7th European Community Framework Programme.

References

[1] S. Nemat-Nasser, M. Hori: *Micromechanics: overall properties of heterogeneous materials* (North-Holland, Elsevier, The Netherlands, 1999).
[2] T.I. Zohdi and P. Wriggers: *An introduction to computational micromechanics*, (Springer, Berlin, 2005).
[3] B.L. Adams and T. Olson: Prog Mater Sci, Vol. 43, (1998), p. 1.
[4] A.G. Crocker, P.E.J. Flewitt, and G.E. Smith: Int Mater Rev, Vol. 50(2), (2005), p. 99.
[5] K.M. Döbrich, C. Rau, and C.E. Krill III: Metall Mater Trans A, Vol. 35A, (2004), p. 1953.
[6] M.A. Groeber et al.: Mater Charac, Vol. 57, (2006), p. 259.
[7] G.K. Sfantos and M.H. Aliabadi: Int J Numer Meth Eng, Vol. 69, (2007), p. 1590.
[8] F. Fritzen, T. Böhlke and E. Schnack: Comput Mech, Vol. 43, (2009), p. 701.
[9] R. Quey, P.R. Dawson, and F. Barbe: Comput Meth App Mech Eng, Vol. 200, (2011), p. 1729.
[10] N.A. Schclar: *Anisotropic analysis using boundary elements*, (Computational Mechanics Publications, Southampton, 1994).
[11] M.H. Aliabadi: *The boundary element method: applications in solids and structures*, (John Wiley & Sons Ltd, England, 2002).
[12] J.R. Shewchuk: in Applied Computational Geometry: Towards Geometric Engineering, ed. M.C. Lin and D. Manocha, vol. 1148 of Lecture Notes in Computer Science, Springer-Verlag, Berlin, (1996).
[13] T. Kanit et. al: Int J Solids Struct, Vol. 40, (2003), p. 3647.
[14] **.** Arlt and G.R. Schodder, Journal of the Acoustical Society of America, Vol. 37(2), (1965) p.384.
[15] W.R.L. Lambrecht, B. Segall, M. Methfessel, M. van Schilfgaarde. Physical Review B, Vol. 44(8), (1991), p.3685.
[16] R.D. Carnahan, Journal of the American Ceramic Society, Vol. 51(4), (1968), p.223.